Table II. Zero-Field Splitting Parameters for $(nor)_4Cr$ in Isooctane at 93°K

Conformn	D, cm^{-1}	E, cm^{-1}	Conformn	D, cm^{-1}	E, cm^{-1}
I	0.027	0.0041	III	0.013	0.0032
II	0.023	0.0027	IV	0.012	0.0029

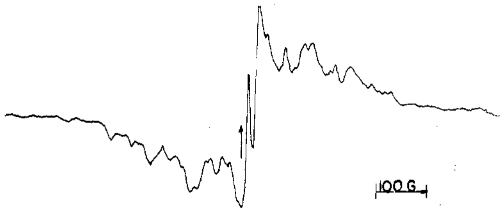

Figure 4. Epr spectrum of $(nor)_4Cr$ 0.32 m*M* in isooctane at 77°K, $\Delta m = 1$ transition. Marker is for DPPH.

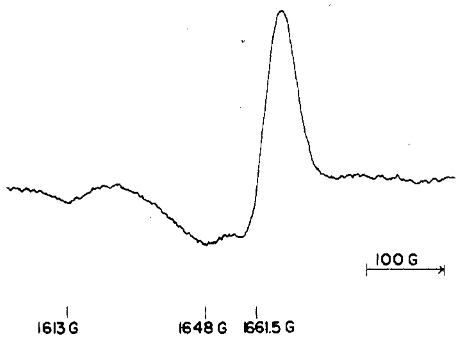

Figure 5. Epr spectrum of $(nor)_4Cr$ 0.32 m*M* in isooctane at 77°K, $\Delta m = 2$ transition.

quantum transition was not observed even at 200 mW. This situation is only possible if $D \approx -3E$ in eq 10.

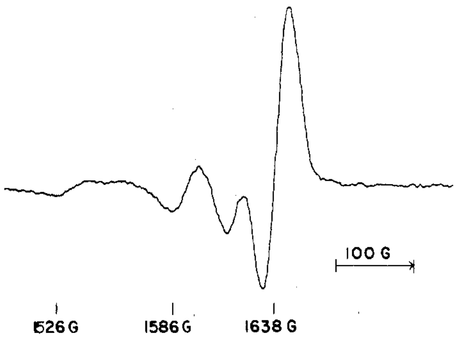

Figure 6. Epr spectrum of $(nor)_4Cr$ 1.85 m*M* in cyclohexane at 77°K, $\Delta m = 2$ transitions.

Since isooctane was the first solvent noted by us to perturb the symmetry of the $(nor)_4Cr$ molecule, several other solvents were examined. Their choice was based on structural similarities to isooctane. Therefore, 2,2-dimethylheptane resembles one end of the isooctane molecule and 2-methylheptane and 2-methylpentane resemble the other end. It is only in the case of 2,2-dimethylheptane that there is a hint of zero-field splitting of its $\Delta m = 1$ transition. Apparently, there is no relationship between the shape of the solvent molecule and its effect on the zero-field splitting of $(nor)_4Cr$. Also most of the alphatic hydrocarbons probably have the same glass transition temperatures of 80-90°K.[20] According to the significant structure theory of liquids[21] the viscosities of these glasses would be comparable. It is possible that the phenomenon described here is of a local nature.

Acknowledgment. This work was supported by Grant No. GH 39111 from the National Science Foundation.

Registry No. $(nor)_4Cr$, 36333-78-5; 2,2-dichloronorbornane, 19916-65-5; 1-chloronorbornane, 765-67-3; $CrCl_3 \cdot 3THF$, 10170-68-0.

(20) W. Kauzmann, *Chem. Rev.*, 43, 219 (1948).

(21) G. L. Faerber, S. W. Kim, and H. Eyring, *J. Phys. Chem.*, 74, 3510 (1970).

Contribution from the Institute of Chemistry, University of Wroclaw, 50-383 Wroclaw, Poland

Syntheses, Infrared Spectra, Magnetic Properties, and Electronic Structures of Di-μ-oxo- and Di-μ-oxo-bis(di-μ-oxo)-Bridged Oxomolybdates(V) and Their Theoretical Interpretation

BOGUSLAWA JEZOWSKA-TRZEBIATOWSKA,* MIKOLAJ F. RUDOLF, LESZEK NATKANIEC, and HELENA SABAT

Received May 1, 1973

The studies of several dimeric and tetrameric oxomolybdates(V) are reported. By the appropriate synthesis routes double-bridged di-μ-oxo-bis[oxomolybdates(V)], μ-oxo-μ-(sulfato,perchlorato,oxalato)-bis[oxomolybdates(V)], and tetrameric di-μ-oxo-bis[di-μ-oxo-oxodimolybdates(V)] were obtained. The character of molybdenum-oxygen bonding is discussed in detail, based on the normal-coordinate analysis carried out for the dimeric di-μ-oxo-bridged oxomolybdates(V) and for a simplified model of the oxomolybdate(V) tetramers. The electronic structure calculations for the dimeric double-bridged $[Mo_2O_4Cl_4(H_2O)_2]^{2-}$ and single-bridged $[Mo_2O_3(NCS)_8]^{4-}$ complexes, carried out by the SCCC MO and angular overlap methods, respectively, are reported. On the basis of these results the origin of the spin pairing in polymeric oxomolybdates(V) is discussed in detail.

Introduction

Metal-metal interaction has become the subject of intensive studies in recent years.

Depending on the geometrical configuration of a molecule and on the electronic structure of a metal ion, the metal-metal interaction between paramagnetic ions could be weak (exchange interaction) or strong (bonding interaction), indirect (interaction involving the diamagnetic atoms or bridging molecules) or direct as observed in metal-metal bonded polynuclear complexes.

The metal-metal interaction may be observed in (a) bi- and polynuclear complexes in which metal atoms are bridged by simple bridging groups such as O^{2-}, OH^-, NH_2^-, Cl^-, and S^{2-}; (b) bi- and polynuclear complexes in which metal atoms are bridged either by molecules, *e.g.*, β-diketonates and Schiff bases, or by complex anions such as carboxylates and their derivatives; and (c) bi- and polynuclear complexes in which metal atoms are linked directly by metal-metal bonding. In many cases, however, the nature of metal-metal interaction cannot be stated explicitly, since various couplings (different in their mechanisms and strengths) occur and determine the magnetic properties of a system.

In the present paper we report the results of studies on magnetic properties of a large group of polynuclear oxomolybdates(V). Due to the geometrical configuration of bridging groups several kinds of strong metal-metal bonding interactions are observed.

Experimental Section

Preparation of Compounds. Ammonium, pyridinium, and tetramethylammonium oxopentachloromolybdates(V), I, were prepared as reported by James, *et al.*[1] Ammonium oxopentabromomolybdate(V), II, and pyridinium oxotetrabromoaquomolybdate(V), III, were synthesized according to the method of Allen, *et at.*[2]

Ammonium Di-μ-oxo-bis(oxochlorohydroxoaquomolybdate(V)), $(NH_4)_2[Mo_2O_4Cl_2(OH)_2(H_2O)_2]$, IV. Ammonium oxopentachloromolybdate(V) (0.01 mol) was dissolved in 20 ml of MeOH and followed by addition of 0.36 ml of water. To the resulting deep green solution potassium bicarbonate (0.03 mol) was added in small portions. After complete reaction, the red solution was filtered to remove alkali chlorides, 10 ml of dioxane was added, and the resulting solution was cooled to −10°, held at this temperature for 3 hr, and filtered again. The filtrate was evaporated under reduced pressure to a volume of 15 ml, filtered again, and evaporated to dryness. The brick-red microcrystalline complex was dried *in vacuo* at 50°. The complex was found to be insoluble in common organic solvents. Aqueous solutions of IV were slowly hydrolyzed yielding $MoO(OH)_3$.

Pyridinium Di-μ-oxo-bis(oxodichloroaquomolybdate(V)), $(PyrH)_2[Mo_2O_4Cl_4(H_2O)_2]$, V. A solution of 0.01 mol of I−pyridinium salt in 10 ml of absolute MeOH and 0.36 ml of water followed by dropwise addition of 0.02 mol of pyridine was vigorously stirred. After some minutes large, brick red crystals of V separated from solution. These crystals were collected, washed with 15 ml of MeOH, and finally dried *in vacuo* over P_2O_5. The complex is slightly soluble in MeOH. Aqueous solutions of V are unstable.

In a similar way the tetramethylammonium di-μ-oxo-bis(oxodichloroaquomolybdate(V)), VI, and pyridinium di-μ-oxo-bis(oxodibromoaquomolybdate(V)), VII, were obtained starting from I−tetramethylammonium salt and III, respectively.

Pyridinium Di-μ-oxo-bis(oxochlorodihydroxomolybdate(V)), $(PyrH)_4[Mo_2O_4Cl_2(OH)_4]$, VIII. This complex was obtained similarly to V using 0.04 mol of pyridine. The orange microcrystalline complex is insoluble in common organic solvents. Aqueous solutions of VIII are completely hydrolyzed yielding $MoO(OH)_3$.

Pyridinium Di-μ-oxo-bis(di-μ-oxo-oxotetrachloroaquodimolybdate(V)), $(PyrH)_4[Mo_4O_8Cl_8(H_2O)_2]$, IX. A solution of I−pyridinium salt (0.01 mol) in 30 ml of EtOH (96%) was refluxed for 15 min and 15 ml of dioxane was added. An amorphous pink precipitate was formed which was filtered after 1 hr and washed several times with EtOH (96%) and finally dried *in vacuo* over P_2O_5. This complex, in contrast to V, is insoluble in MeOH and only slightly soluble in water with total decomposition.

Pyridinium Di-μ-oxo-bis(di-μ-oxo-oxotetrabromoaquodimolybdate(V)), $(PyrH)_4[Mo_4O_8Br_8(H_2O)_2]$, X, was prepared by the above given method using III as the starting material.

Pyridinium [Di-μ-oxo-oxotetrachloroaquodimolybdate(V)]-di-μ-oxo-[di-μ-oxo-oxotetrachlorohydroxodimolybdate(V)], $(PyrH)_5$-$[Mo_4O_8Cl_8(OH)(H_2O)]$, XI. Compound I−pyridinium salt (0.01 mol) was dissolved in 10 ml of absolute MeOH and 15 ml of dioxane containing 0.36 ml of water was added. Under continuous stirring 0.02 mol of pyridine was added dropwise. After 3 min, fine copper red crystals began to form in the red solution. The residue was filtered after 2 hr, and the complex obtained was washed several times with small amounts of MeOH–dioxane mixture (1:1) followed by dry diethyl ether and finally dried *in vacuo*. The obtained bordeaux red complex is insoluble in common organic solvents.

Pyridinium [Di-μ-oxo-oxotetrabromoaquodimolybdate(V)]-di-μ-oxo-[di-μ-oxotetrabromohydroxodimolybdate(V)], $(PyrH)_5$-$[Mo_4O_8Br_8(OH)(H_2O)]$, XII. The compound was prepared by the above given method using III as the starting material. After 2 hr very thin copper red needles of the product began to crystallize from the reaction mixture. The crystals were filtered, washed, and dried as XI.

Pyridinium Di-μ-oxo-bis(oxotris(isothiocyanato)molybdate(V)), $(PyrH)_4[Mo_2O_4(NCS)_6]$, XIII, was prepared as reported previously.[3]

Pyridinium μ-Oxo-bis(oxotetrakis(isothiocyanato)molybdate(V)), $(PyrH)_4[Mo_2O_3(NCS)_8]$, XIV. A solution of 2.3 g of ammonium thiocyanate in 4 ml of water was added at 60° to a solution of 4.5 g of I−pyridinium salt in 50 ml of water. From the resulting purple-red solution a black oil was separated which crystallized after 24 hr at room temperature. The resulting solid was filtered and washed several times with water and finally dried *in vacuo* over P_2O_5. The purple-red amorphous complex is soluble in acetone, yielding purple-red, unstable solutions. On crystallization from MeOH, XIV undergoes total decomposition yielding XIII.

Pyridinium μ-Oxo-μ-sulfato-bis(oxotris(isothiocyanato) molybdate(V)), $(PyrH)_4[Mo_2O_3(SO_4)(NCS)_6]$, XV. Compound XIII (2.3 g) was stirred for 30 min with 60 ml of 20% sulfuric acid at room temperature. After 30 min a black oil was separated from the purple-red solution. The oil crystallized yielding an amorphous, water-insoluble precipitate. The resulting complex was washed after filtration with 50 ml of 20% sulfuric acid, 70 ml of water, 100 ml of MeOH, and finally dry diethyl ether; mp 204° dec. Compound XV is soluble in acetone yielding unstable, purple-red solutions.

Pyridinium μ-Oxo-μ-perchlorato-bis(oxotris(isothiocyanato)-molybdate(V)), $(PyrH)_3[Mo_2O_3(ClO_4)(NCS)_6]$, XVI. Compound XIII (5.0 g) was stirred for 2.5 hr with 30 ml of 20% perchloric acid at room temperature. The starting XIII dissolved completely and after some minutes a black heavy oil was formed which crystallized after about 30 min. After filtration the reaction product was washed with 50 ml of 20% perchloric acid, with water, three times with 30 ml of dioxane, and finally with dry diethyl ether. The product was dried *in vacuo* over KOH. XVI forms an amorphous, purple-violet powder, mp 154–156° dec. XVI is quite soluble in acetone giving unstable, purple-red solutions.

Pyridinium μ-Oxo-μ-oxalato-bis(oxotris(isothiocyanato)molybdate-(V)), $(PyrH)_4[Mo_2O_3(C_2O_4)(NCS)_6]$, XVII. Compound XIII (4.0 g) was stirred for 1 hr with 60 ml of oxalic acid (20% aqueous solution) at 70°. The resulting dark red-brown solution was filtered and the filtrate was allowed to crystallize at room temperature. XVII crystallizes in the from of violet-red thin plates which after filtration were washed several times with absolute MeOH to remove the excess of oxalic acid and dried *in vacuo* over KOH.

Analytical Methods. The molybdenum contents of the oxomolybdates(V) were determined gravimetrically by ignition of the molybdenyl oxinate, precipitated from solutions at pH 4.5 in the presence of H_2O_2 at 70°, to MoO_3 at 550°.[4] The oxidation numbers of molybdenum in these complexes were determined by cerometric titrations. The halogenide contents were determined by argentometric titrations using the potentiometric method. The contents of thiocyanate and sulfate ions were determined gravimetrically as $BaSO_4$.[5] The carbon, hydrogen and nitrogen contents were determined by the microanalytical methods. The analytical data for the prepared oxomolybdates(V) are collected in Table I.

Physical Measurements. The magnetic susceptibility measurements were carried out in the temperature range 77–300°K using the Gouy method. Measurements at several different field strengths (H_{max} = 12 kOe) were made at each temperature but no field strength dependences were observed for any one of the complexes. Infrared spectra were obtained using Perkin-Elmer Model 621 and Carl-Zeiss Jena UR-20 spectrophotometers. The measurements were carried out on both Nujol and hexachlorobutadiene mulls and on KBr disks in the range 200–3500 cm^{-1}. No differences between the spectra of mulls and those of the disks were observed.

---

(1) R. G. James and W. Wardlaw, *J. Chem. Soc.*, 2145 (1927).

(2) J. F. Allen and H. M. Neumann, *Inorg. Chem.*, 3, 1612 (1964).

(3) L. F. Audrieth, *Inorg. Syn.*, 3, 160 (1950).

(4) (a) R. Pribil and M. Malat, *Collect. Czech. Chem. Commun.*, 15, 120 (1950); (b) M. Malinek, *Chem. Listy*, 48, 30 (1954).

(5) A. J. Vogel, "Text-Book of Quantitative Inorganic Analysis," Longmans, Green and Co., New York, N. Y., 1961.

Table I. Analytical Data for Polynuclear Oxomolybdates(V)

	% C		% H		% N		% Cl (Br)		% S		% Mo	
Compd	Calcd	Found	Calcd	Found	Calcd	Found	Calcd	Found	Calcd	Found	Calcd	Found
IV					16.47	16.28	16.43	16.58			44.34	44.31
V	20.22	20.35	2.69	2.32	4.72	4.93	23.88	23.71			32.32	32.28
VI	16.51	16.32	4.81	4.50	4.81	4.68	24.37	24.11			32.99	33.21
VII	15.56	15.38	2.07	2.32	3.63	4.40	41.42	41.69			24.87	25.13
VIII	33.59	33.76	3.92	3.56	7.46	7.39	9.44	9.45			25.55	25.45
IX	20.86	20.73	2.43	2.18	4.86	4.87	24.63	24.95			33.33	33.24
X	15.94	15.90	1.86	1.73	3.72	3.50	42.42	42.05			25.47	25.63
XI	24.40	24.56	2.68	2.73	5.69	5.54	23.00	23.13			31.20	30.83
XII	19.10	19.13	2.10	1.86	4.52	4.49	40.66	40.19			24.41	24.06
XIII	33.78	33.59	2.60	2.88	15.14	14.99			20.81	20.92	20.77	20.76
XIV	32.82	32.51	2.34	2.87	16.41	16.10			25.03	25.34	18.74	18.55
XV	31.08	31.17	2.39	2.53	13.95	14.04			22.34	22.53	19.10	19.13
XVI	27.18	27.03	1.94	2.08	13.58	13.61	3.82	3.72	20.73	20.73	20.68	20.71
XVII	33.74	33.62	2.41	2.53	14.05	14.13			19.30	19.36	19.25	19.21

Table II. Magnetic Susceptibilities of Some Bi- and Tetranuclear Oxygen-Bridged Oxomolybdates(V)

$(PyrH)_2[Mo_2O_4Cl_4(H_2O)_2]$							
T, °K	91.0	103.5	123.0	140.0	161.0	178.0	200.0
$10^6\chi_M$, cgsu	751	336	273	257	199	155	166
T, °K	238.0	270.0	294.5				
$10^6\chi_M$, cgsu	178	148	157				
$(PyrH)_4[Mo_4O_8Cl_8(H_2O)_2]$							
T, °K	90.0	101.0	120.0	137.0	144.0	162.0	178.0
$10^6\chi_M$, cgsu	715	704	644	506	492	522	516
T, °K	202.0	221.0	236.0	258.0	275.0	296.0	
$10^6\chi_M$, cgsu	501	536	515	509	521	508	
$(PyrH)_4[Mo_2O_3(NCS)_8]$							
T, °K	83.0	100.0	115.0	128.0	147.0	168.0	187.0
$10^6\chi_M$, cgsu	209	220	173	152	148	151	142
T, °K	203.0	232.0	254.0	270.0	290.0	308.0	318.0
$10^6\chi_M$, cgsu	132	107	114	120	127	198	166
T, °K	328.0	339.0	345.0	355.0	365.0	374.0	389.0
$10^6\chi_M$, cgsu	147	164	202	240	201	161	121
T, °K	400.0	410.0					
$10^6\chi_M$, cgsu	141	165					
$(PyrH)_4[Mo_2O_3(SO_4)(NCS)_6]$							
T, °K	77.0	89.5	102.5	117.0	130.5	144.5	158.5
$10^6\chi_M$, cgsu	−66	75	3	−30	−23	228	188
T, °K	172.0	185.5	202.0	214.0	228.0	245.0	257.0
$10^6\chi_M$, cgsu	157	145	160	125	44	50	−6
T, °K	274.5	287.0	296.5				
$10^6\chi_M$, cgsu	100	64	−19				
$(PyrH)_3[Mo_2O_3(ClO_4)(NCS)_6]$							
T, °K	77.0	90.0	103.0	117.0	132.0	147.0	162.0
$10^6\chi_M$, cgsu	873	872	712	627	590	593	565
T, °K	175.0	183.5	203.0	215.0	234.0	250.0	260.5
$10^6\chi_M$, cgsu	558	641	739	415	274	201	227
T, °K	273.5	288.0	294.5				
$10^6\chi_M$, cgsu	227	200	207				
$(PyrH)_4[Mo_2O_3(C_2O_4)(NCS)_6]$							
T, °K	77.0	89.5	104.5	119.5	133.5	150.0	160.0
$10^6\chi_M$, cgsu	179	103	112	59	4	125	−23
T, °K	184.0	201.0	219.5	234.0	251.5	283.5	288.0
$10^6\chi_M$, cgsu	145	98	270	34	−22	−98	−79

Results

Magnetic Susceptibilities. The results of magnetic susceptibility measurements are given in Table II. Because of the nearly temperature-independent and small values of the magnetic susceptibilities no magnetic moments were calculated for individual complexes. The molar susceptibilities were calculated for the whole molecules of dimers and tetramers taking the appropriate diamagnetic corrections into account. In Table II the data for the most representative compounds are given. The magnetic susceptibilities of the remaining complexes cover the range (74–281) × 10^{-6} cgsu (room-temperature values) and are also practically temperature independent.

Infrared Spectra. The results of ir spectral measurements are given in Tables III–V. The characteristic frequencies of the outer-sphere cation vibrations, as well as the frequencies due to deformation and stretching modes of the OH groups, have been omitted.

Theory

Assumptions. Because of the lack of X-ray data for the dimeric oxomolybdates(V) studied, we have taken the data reported for monomeric oxohalomolybdates(V) for the bond length and bond angles. Also the X-ray data of three structurally similar dimeric di-μ-oxo-oxomolybdates(V) were taken into account.[6-10] The electronic structure calculations for the dimeric di-μ-oxo-bis(oxodichloroaquomolybdate(V)) ion were carried out assuming that all valence angles are 90° and that the complex has C_{2h} symmetry. The bond distances were assumed to be close to the following: Mo–O_t, 1.67 Å; Mo–O (H_2O), 2.27 Å; Mo–O_b, 1.90 Å; Mo–Cl, 2.405 Å; Mo–Br, 2.565 Å. The assumed molecular model of this complex is shown in Figure 1.

SCCC MO Calculations.[11] To explain the electronic structure of di-μ-oxo-bridged oxomolybdates(V), the SCCC MO method was applied to the di-μ-oxo-bis(oxodichloroaquomolybdate(V)) $[Mo_2O_4Cl_4(H_2O)_2]^{2-}$ ion taking the above given assumptions into account.[12]

All molybdenum 5s, 5p, 4d and ligand *n*s, *n*p valence orbitals were taken into account. The valence orbitals of oxygen atoms of water molecules were approximated by the tetrahedral hybrid functions (sp^3). For the calculations of the group overlap integrals the analytical expressions for the orbitals of Mo^+, Cl^0, and O^0 reported by Basch and Gray,[13] Freeman and Watson,[14] and Ballhausen and Gray,[15] respectively, were used. The diagonal matrix elements were approximated as reported by Golebiewski and Kowalski[16] for

---

(6) T. Glowiak, M. Kubiak, and T. Lis, *Proc. Int. Conf. Coord. Chem., 13th*, 2, 372 (1970).

(7) I. G. Scane, *Acta Crystallogr.*, 23, 85 (1967).

(8) F. A. Cotton and S. M. Morehouse, *Inorg. Chem.*, 4, 1377 (1965).

(9) J. R. Knox and C. K. Prout, *Acta Crystallogr., Sect. B*, 25, 1857 (1969).

(10) L. T. J. Delbaere and C. K. Prout, *Chem. Commun.*, 162 (1971).

(11) H. Basch, A. Viste, and H. B. Gray, *J. Chem. Phys.*, 44, 10 (1966).

(12) L. Natkaniec, M. F. Rudolf, and B. Jezowska-Trzebiatowska, *Theoret. Chim. Acta*, 28, 193 (1973).

(13) H. Basch and H. B. Gray, *Theoret. Chim. Acta*, 4, 367 (1966).

(14) A. J. Freeman and R. E. Watson, *Phys. Rev.*, 123, 521 (1961).

(15) C. J. Ballhausen and H. B. Gray, *Inorg. Chem.*, 1, 111 (1962).

(16) A. Golebiewski and H. Kowalski, *Theoret. Chim. Acta*, 12, 293 (1968).

Table III. Characteristic Frequencies of Dimeric Di-μ-oxo-Bridged Oxomolybdates(V)[a]

$(NH_4)_2[Mo_2O_4Cl_2(OH)_2(H_2O)_2]$
312 s, 350 m, 470 s, b, 510 sh, 550 m, 715 s, 740 s, b, 968 vs

$(PyrH)_2[Mo_2O_4Cl_4(H_2O)_2]$
282 vw, 303 vw, 320 s, 345 m, 505 s, 522 vs, 732 vs, 750 vs (Pyr), 968 s, 988 vs

$(Me_4N)_2[Mo_2O_4Cl_4(H_2O)_2]$
290 vw, 318 vs, 349 m, 457 w, 487 s, b, 505 s, 683 vs, 732 vs, 940 vs, 985 vs

$(PyrH)_4[Mo_2O_4Cl_2(OH)_4]$
320 vs, b, 372 m, 480 s, b, 488 sh, 510 s, b, 540 s, 730 s, 742 vs (Pyr), 800 m, 950 s, 967 vs, b

$(PyrH)_2[Mo_2O_4Br_4(H_2O)_2]$
231 s, 358 m, 490 s, 550 w, b, 720 vs, 759 vs (Pyr), 958 m, 976 vs

$(PyrH)_4[Mo_2O_4(NCS)_6]$
292 m,[b] 315 m,[b] 457 m,[c] 500 m, 721 vs, 746 vs (Pyr), 951 vs, 2060 vs[d]

$K_2[Mo_2O_4(C_2O_4)_2(H_2O)_2]\cdot 3H_2O$
487 m,[e] 527 m, b, 740 s, 800 s,[f] 963 s

[a] Frequencies are given in cm^{-1}. Intensity key: v, very; s, strong; m, medium; w, weak; sh, shoulder; b, broad. [b] ν(Mo–N) stretch. [c] δ(NCS) deformation mode. [d] ν(C≡N) stretch. [e] ν(Mo–O (C_2O_4)) stretch. [f] δ(O–C=O) + ν((Mo–O) (C_2O_4)).

Table IV. Characteristic Frequencies of Tetrameric Di-μ-oxo-bis[di-μ-oxo-(oxodimolybdates(V))][a]

$(PyrH)_4[Mo_4O_8Cl_8(H_2O)_2]$
235 s, 295 vs, 510 vs, 565 w, 610 w, *721 vs*, 737 vs, 750 vs (Pyr), *888 vs, b, 968 vw*

$(PyrH)_5[Mo_4O_8Cl_8(OH)(H_2O)]$
233 m, 273 s, 290 s, 326 vs, 513 vs, 608 w, 615 w, *722 vs*, 737 vs, 749 vs (Pyr), *885 vs, b, 978 vw*

$(PyrH)_4[Mo_4O_8Br_8(H_2O)_2]$
494 vs, *713 vs*, 726 vs, 740 vs (Pyr), *880 vs, b, 970 vw*

$(PyrH)_5[Mo_4O_8Br_8(OH)(H_2O)]$
495 vs, *715 vs*, 728 vs, 746 vs (Pyr), *880 vs, b*

[a] Frequencies are given in cm^{-1}. Intensity key: v, very, s, strong; m, medium; sh, shoulder; b, broad.

Table V. Characteristic Frequencies of μ-Oxo-Bridged and Hetero-Bridged Binuclear Oxomolybdates(V)[a]

$(PyrH)_4[Mo_2O_3(NCS)_8]$
320 s,[b] 470 m,[c] 480 sh,[c] 742 s (Pyr), 868 sh, 873 w, 955s, 2035 vs,[d] 2050 sh[d]

$(PyrH)_4[Mo_2O_3(SO_4)(NCS)_6]$
290 m,[b] 310 sh,[b] 419 m,[e] 435 s, 480 m,[c] 592 w, 665 m, 742 s (Pyr), 785 m, 956 s, 1008 m,[f] 1075 s,[g] 1100 s,[g] 1175 vs,[g] 2050 vs, b[d]

$(PyrH)_3[Mo_2O_3(ClO_4)(NCS)_6]$
280 m, 300 sh,[b] 320 m,[b] 349 s,[e] 443 s, 476 w, 487 s,[c] 618 w,[h] 740 vs (Pyr), 785 m, 945 w, 971 vs, 981 vs, 1079 s,[g] 1098 s,[g] 1113 vs,[g] 2045 vs, b[d]

$(PyrH)_4[Mo_2O_3(C_2O_4)(NCS)_6]$
295 s,[b] 345 s, 360 m,[i] 439 s, 475 s,[c] 490 sh,[c] 535 m, 747 s (Pyr), 750 s, 790 s,[j] 810 s,[j] 908 s,[k] 963 s, 1670 vs, 2050 vs, b[d]

[a] Frequencies are given in cm^{-1}. Intensity key: v, very; s, strong; m, medium; w, weak; sh, shoulder; b, broad. [b] ν(Mo–N) stretch. [c] δ(NCS) deformation mode. [d] ν(C≡N) stretch. [e] ν(Mo–O (MO_4)) stretch. [f] $\nu_1(MO_4)$. [g] $\nu_3(MO_4)$ stretch. [h] $\nu_4(MO_4)$ stretch. [i] ν(Mo–O (C_2O_4)) stretch. [j] δ(O=C–O) + ν(Mo–O (C_2O_4)). [k] ν_s(C–O) + δ(O=C–O).

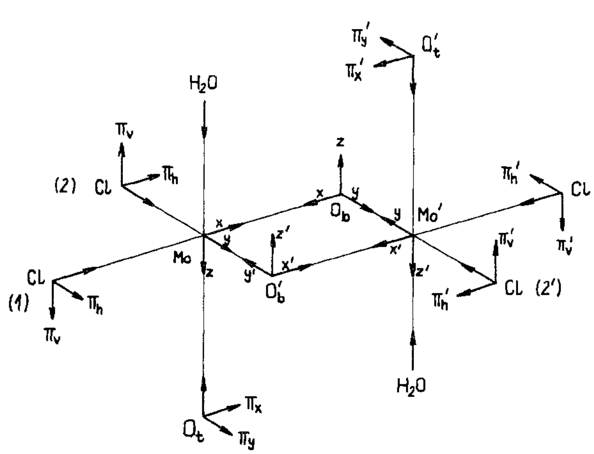

Figure 1. Molecular model of the $[Mo_2O_4Cl_4(H_2O)_2]^{2-}$ ion.

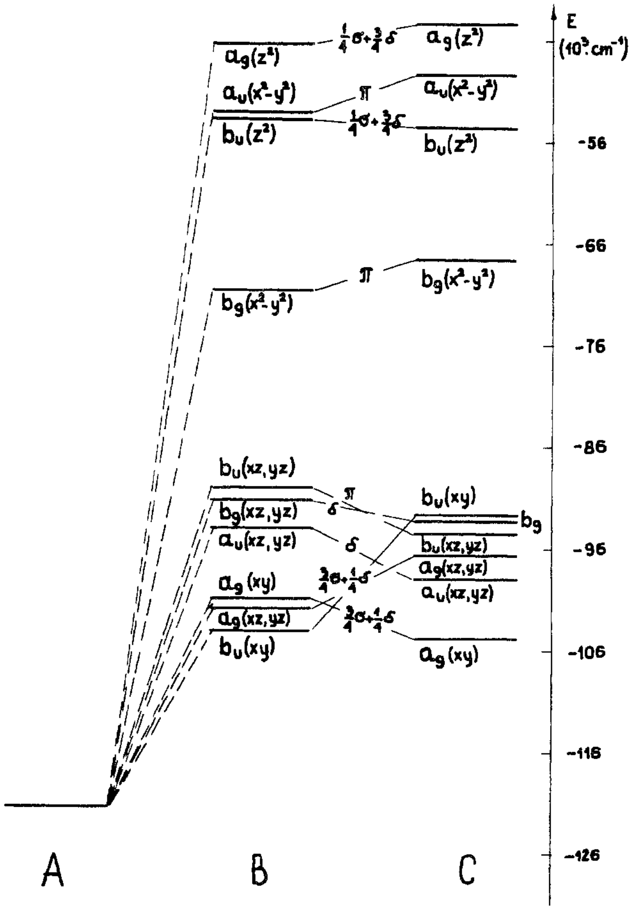

Figure 2. MO diagram of the $[Mo_2O_4Cl_4(H_2O)_2]^{2-}$ ion. The MO's consisting mainly of molybdenum d orbitals are shown: (A) molybdenum d orbitals; (B) A + Mo–O_t, Mo–O_b, Mo–O_{H_2O}, and Mo–Cl interactions; (C) B + Mo–Mo interaction. The symbols σ, π, and δ denote the types of metal–metal interactions resulting from the diagonal matrix elements (see ref 11).

molybdenum and by Viste and Gray[17] for the ligand orbitals. The energy calculations were carried out successively taking all possible metal–ligand and metal–metal interactions into account: (a) only the Mo–O_t, Mo–O (H_2O), and Mo–Cl interactions being considered; (b) a + Mo–O_b interaction being considered; (c) b + Mo–Mo interaction being considered. In all variants of calculations the ligand–ligand overlap corrections were considered. The results of calculations are given in Table VI and shown in Figure 2.

Angular Overlap Model Calculations. The infrared spectral studies of the pyridinium μ-oxo-bis(oxotetrakis(isothiocyanato)molybdate(V)) indicate the presence of a practically

---

[17] A. Viste and H. B. Gray, *Inorg. Chem.*, 3, 1113 (1964).

Table VI. Energies and Symmetries of Molecular Orbitals of the $[Mo_2O_4Cl_4(H_2O)_2]^{2-}$ Ion[a]

Energy	Symmetry	Contribution of molybdenum and ligand orbitals
−276.1	$1a_g$	s_{O_b} (0.487), s_{O_t} (0.448)
−264.3	$1b_u$	s_{O_t} (0.968)
−262.8	$1a_u$	s_{O_b} (0.958)
−259.1	$2a_g$	s_{O_t} (0.480), s_{O_b} (0.432)
−208.5	$3a_g$	s_{Cl} (0.914)
−207.1	$2b_u$	s_{Cl} (0.976)
−205.2	$2a_u$	s_{Cl} (0.943)
−204.2	$1b_g$	s_{Cl} (0.963)
−160.6	$3b_u$	σ_{H_2O} (0.488), d_{xz} (0.145), $p_{z_{O_b}}$ (0.122)
−158.7	$4a_g$	σ_{H_2O} (0.583)
−151.0	$5a_g$	$p_{x_{O_b}}$ (0.410), d_{xy} (0.343)
−150.8	$4b_u$	d_{xz} (0.229), $p_{\sigma_{O_t}}$ (0.220), σ_{H_2O} (0.192), π_x (0.132)
−150.7	$2b_g$	d_{xz} (0.348), π_x (0.290), $p_{z_{O_b}}$ (0.286)
−143.8	$5b_u$	$p_{x_{O_b}}$ (0.423), $p_{\sigma_{Cl}}$ (0.139), d_{xy} (0.119)
−141.4	$6a_g$	$p_{\sigma_{O_t}}$ (0.705)
−139.6	$3a_u$	π_x (0.505), d_{xz} (0.309)
−139.3	$6b_u$	$p_{\sigma_{O_t}}$ (0.584)
−136.4	$3b_g$	$p_{x_{O_b}}$ (0.661), $d_{x^2-y^2}$ (0.252)
−136.1	$4a_u$	$p_{x_{O_b}}$ (0.415), $d_{x^2-y^2}$ (0.228), $p_{\sigma_{Cl}}$ (0.202)
−135.4	$7a_g$	$p_{\sigma_{Cl}}$ (0.360), π_x (0.286)
−127.4	$4b_g$	$p_{\sigma_{Cl}}$ (0.543), $d_{x^2-y^2}$ (0.148)
−125.8	$8a_g$	$p_{\sigma_{Cl}}$ (0.384), π_x (0.229), d_{xz} (0.191)
−127.0	$7b_u$	$p_{\sigma_{Cl}}$ (0.539), π_h (0.135)
−119.8	$5a_u$	$p_{\sigma_{Cl}}$ (0.428), $p_{x_{O_b}}$ (0.396)
−118.3	$5b_g$	π_x (0.286), $p_{z_{O_b}}$ (0.250), $p_{\sigma_{Cl}}$ (0.177), π_v (0.149)
−117.0	$8b_u$	$p_{z_{O_b}}$ (0.485), π_x (0.178)
−116.9	$9a_g$	π_h (0.473), $p_{x_{O_b}}$ (0.261), d_{xy} (0.207)
−110.4	$9b_u$	π_h (0.473), π_v (0.324)
−109.7	$10a_g$	π_v (0.862)
−108.2	$10b_u$	π_v (0.466), π_h (0.200)
−108.2	$6a_u$	π_v (0.849)
−106.2	$7a_u$	π_h (0.982)
−105.5	$6b_g$	π_h (0.952)
−105.2	$11a_g$	π_h (0.471), d_{xy} (0.367), $p_{x_{O_b}}$ (0.138)
−102.2	$7b_g$	π_v (0.620), d_{xz} (0.150), π_x (0.137)
−99.3	$8a_u$	d_{xz} (0.532), π_x (0.319)
−97.1	$12a_g$	d_{xz} (0.684), π_x (0.225)
−94.8	$11b_u$	d_{xz} (0.490), π_x (0.269), $p_{z_{O_b}}$ (0.144)
−93.7	$8b_g$	d_{xz} (0.430), $p_{z_{O_b}}$ (0.269), π_x (0.148), π_v (0.133)
−93.1	$12b_u$	d_{xy} (0.701), $p_{x_{O_b}}$ (0.203)
−68.0	$9b_g$	$d_{x^2-y^2}$ (0.551), $p_{\sigma_{Cl}}$ (0.217), $p_{x_{O_b}}$ (0.193)
−54.9	$13b_u$	d_{z^2} (0.521), $p_{z_{Mo}}$ (0.124), σ_{H_2O} (0.123)
−50.1	$9a_u$	$d_{x^2-y^2}$ (0.541), $p_{\sigma_{Cl}}$ (0.196), $p_{x_{O_b}}$ (0.118)
−44.8	$13a_g$	d_{z^2} (0.475), $p_{z_{Mo}}$ (0.190)
12.8	$14b_u$	s_{Mo} (0.501), $p_{z_{Mo}}$ (0.250), $p_{x_{Mo}}$ (0.196)
18.2	$10b_g$	$p_{x_{Mo}}$ (0.953)
30.5	$14a_g$	$p_{z_{Mo}}$ (0.354), $p_{x_{O_b}}$ (0.305)
67.0	$10a_u$	$p_{x_{Mo}}$ (0.892)
74.7	$15b_u$	$p_{x_{Mo}}$ (0.833), s_{Mo} (0.120)
79.8	$15a_g$	$p_{x_{Mo}}$ (0.757)
134.8	$16b_u$	$p_{z_{Mo}}$ (0.575), s_{Mo} (0.326)
168.2	$16a_g$	s_{Mo} (0.488), $p_{z_{Mo}}$ (0.382)

[a] The energies are given in 10^3 cm^{-1}.

linear oxygen bridge in this complex compound. To determine the electronic state of the metal ion, the energies of the molybdenum d orbitals in the μ-oxo-bridged complex of the $Mo_2O_3L_8{}^{m-}$ type were calculated using the angular overlap model.[18]

The structure of the μ-oxo-bis(oxotetrakis(isothiocyanato)-

---

[18] (a) C. K. Jorgensen, R. Pappalardo, and H. H. Schmidtke, *J. Chem. Phys.*, **39**, 1422 (1963); (b) C. E. Schaffer and C. K. Jorgensen, *Mol. Phys.*, **9**, 401 (1965); (c) C. E. Schaffer, *Pure Appl. Chem.*, **24**, 361 (1970).

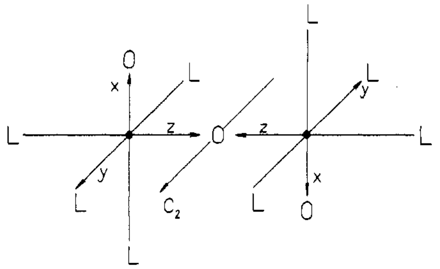

Figure 3. Structure and coordinate system of the $[Mo_2O_3L_8]^{m-}$ ion.

molybdate(V)) ion and the coordinate system used for the calculations are shown in Figure 3.

The energies of molybdenum d orbitals were expressed in terms of AOM parameters similarly as reported by Schmidtke[19] and Glerup.[20] Because of the long Mo-Mo distance (>3.5 Å), the metal-metal interaction was neglected. The off-diagonal matrix element $^3/_4(e^t{}_\sigma + e^L{}_\sigma)$, corresponding to interaction of d_{z^2} and $d_{x^2-y^2}$ orbitals, was also neglected. Taking into account the different symmetries of the 2s and 2p orbitals of the bridging oxygen atom two σ-type AOM parameters $e^b{}_{\sigma_s}$ and $e^b{}_{\sigma_p}$ were set into the calculations (see also ref 19). The energies of the molybdenum d orbitals expressed in terms of AOM parameters are given in Table VII. In this table the results obtained by Schmidtke[19] for the $[L_5M\text{-}O\text{-}ML_5]^{n-}$ complex of D_{4h} symmetry are also presented. Therefore it is possible to demonstrate the effect of ligand L substitution, in the cis O_b position by terminal oxygen atoms (O_t), on the energies of the d orbitals of the metal atom. Because the L (NCS^-) ligand serves as a weak π-donating group, the AOM parameters decrease in the order $e^L{}_\pi \ll e^b{}_\pi < e^t{}_\pi < e^L{}_\sigma < e^b{}_{\sigma_s} < e^b{}_{\sigma_p} < e^t{}_\sigma$. Thus the energy level diagrams of d orbitals of metal atoms in the $[Mo_2OL_{10}]^{n-}$ and $[Mo_2O_3L_8]^{m-}$ complexes are presented in Figure 4.

Normal-Coordinate Analysis. The calculations were carried out using the generalized valence force field (GVF) model for the di-μ-oxo-bis(oxodichloroaquomolybdate(V)) and di-μ-oxo-bis(oxodibromoaquomolybdate(V)) ions. The symmetry of these 12-atom models is C_{2h} (Figure 1). Of the 30 normal modes of vibrations possible, 15 are infrared active ($6\ A_u + 9\ B_u$) and 15 are Raman active ($9\ A_g + 6\ B_g$). The internal coordinates of the $[Mo_2O_4(hal)_4(H_2O)_2]^{2-}$ ions are shown in Figure 5.

The symmetry coordinates of the ir-active vibrations are listed in Appendix A. One redundant coordinate was included in the calculation (B_u species) but in the final results it gives a zero frequency. The normal-coordinate analysis was carried out using the *GF*-matrix method.[21] In addition to diagonal stretching and bending force constants, the calculations included the following interaction force constants: stretch-stretch, stretch-bending, and bending-bending interaction force constants for coordinates having two common atoms. In the construction of the *G*-matrix, only the elements $g_{s_is_j}$, for combinations of the s_is_j internal coordinates, having at least one common atom were considered. The remaining $g_{s_is_j}$ elements were assumed to be zero. The calculated and experimentally determined eigenvalues and main contributions of internal symmetry coordinates S_i in the normal coordinate Q_N belonging to a given vibration of energy λ_N are listed in Table VIII.

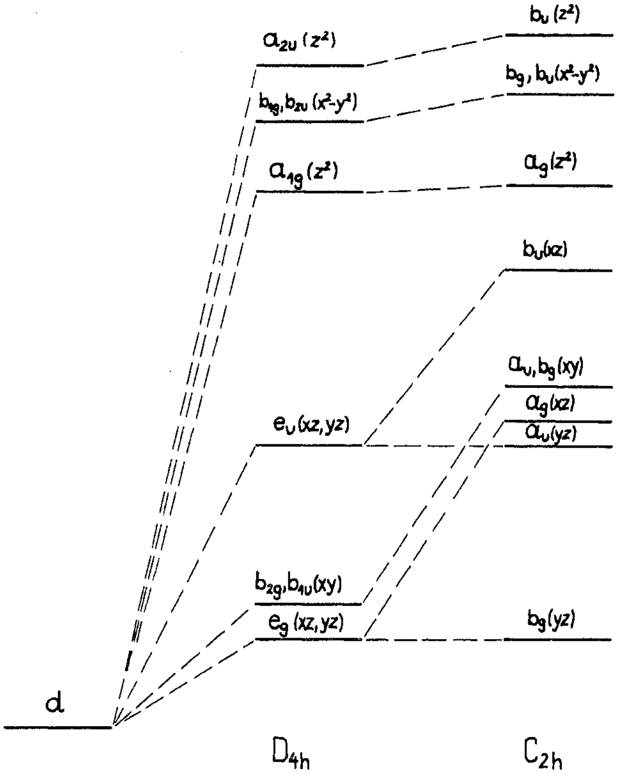

Figure 4. Relative energy diagrams of the $[Mo_2OL_{10}]^{n-}$ and $[Mo_2O_3L_8]^{m-}$ ions resulting from the angular overlap model.

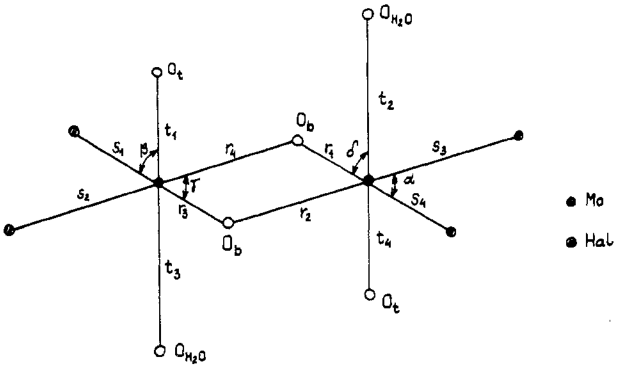

Figure 5. Internal coordinates of the $[Mo_2O_4(hal)_4(H_2O)_2]^{2-}$ ion.

Table VII. Energies of d Orbitals Expressed in AOM Parameters for the $[M_2OL_{10}]^{n-}$ (D_{4h}) and $[M_2O_3L_8]^{m-}$ (C_{2h}) Ions[a]

Combinations of d orbitals	Symmetries and energies of d orbitals			
	D_{4h}		C_{2h}	
$d^+{}_{z^2}$	a_{1g}	$e^b{}_{\sigma_s} + 2e^L{}_\sigma$	a_g	$e^b{}_{\sigma_s} + {}^1/_4e^t{}_\sigma + {}^7/_4e^L{}_\sigma$
$d^-{}_{z^2}$	a_{2u}	$e^b{}_{\sigma_p} + 2e^L{}_\sigma$	b_u	$e^b{}_{\sigma_p} + {}^1/_4e^t{}_\sigma + {}^7/_4e^L{}_\sigma$
$d^+{}_{x^2-y^2}$	b_{1g}	$3e^L{}_\sigma$	a_g	${}^3/_4e^t{}_\sigma + {}^9/_4e^L{}_\sigma$
$d^-{}_{x^2-y^2}$	b_{2u}	$3e^L{}_\sigma$	b_u	${}^3/_4e^t{}_\sigma + {}^9/_4e^L{}_\sigma$
$d^-{}_{xz}$	e_u	$e^b{}_\pi + 3e^L{}_\pi$	b_u	$e^b{}_\pi + e^t{}_\pi + 2e^L{}_\pi$
$d^-{}_{yz}$	e_u	$e^b{}_\pi + 3e^L{}_\pi$	a_u	$e^b{}_\pi + 3e^L{}_\pi$
$d^+{}_{xz}$	e_g	$3e^L{}_\pi$	a_g	$e^t{}_\pi + 2e^L{}_\pi$
$d^+{}_{yz}$	e_g	$3e^L{}_\pi$	b_g	$3e^L{}_\pi$
$d^-{}_{xy}$	b_{1u}	$4e^L{}_\pi$	a_u	$e^t{}_\pi + 3e^L{}_\pi$
$d^+{}_{xy}$	b_{2g}	$4e^L{}_\pi$	b_g	$e^t{}_\pi + 3e^L{}_\pi$

[a] The superscripts L, b, and t denote the AOM parameters of the ligand L, bridge oxygens, and terminal oxygens, respectively.

The ir spectra of tetrameric oxomolybdates(V) show disappearence of the "molybdenyl" stretching frequency (*ca.*

---

(19) H. H. Schmidtke, *Theoret. Chim. Acta*, **20**, 92 (1971).
(20) J. Glerup, *Acta Chem. Scand.*, **26**, 3775 (1972).
(21) E. B. Wilson, J. C. Decius, and P. C. Cross, "Molecular Vibrations," McGraw-Hill, New York, N. Y., 1955.

Table VIII. Energies of A_u and B_u Symmetry Vibrations and Band Assignments of $[Mo_2O_4Cl_4(H_2O)_2]^{2-}$ and $[Mo_2O_4Br_4(H_2O)_2]^{2-}$ Ions[a]

	$[Mo_2O_4Cl_4(H_2O)_2]^{2-}$		$[Mo_2O_4Br_4(H_2O)_2]^{2-}$			
	ν_{exptl}	ν_{calcd}	ν_{exptl}	ν_{calcd}	Contribution of S_i	Type of vibration
A_u	498, 521	502	490	526	S_1 (1.00)	Mo–O_b str
	327	341	219	196	S_2 (1.00), S_4 (0.20)	Mo–Cl(Br) str
		214		96	S_3 (1.00)	(Cl)Br–Mo–O_t def
		102		97	S_6 (1.00)	O_t–Mo–O_b def
B_u	988	976	976	976	S_9 (1.00)	Mo–O_t str
	735	746	720	746	S_7 (1.00)	Mo–O_b str
	370	366	375	366	S_{10} (1.00)	Mo–O_{H_2O} str
	325	341	228	231	S_8 (1.00)	Mo–Cl(Br) str
		202		191	S_{11} (1.00)	Cl(Br)–Mo–(Br)Cl def

[a] Frequencies are given in cm^{-1}. Only the main contributions of S_i internal symmetry coordinates are listed.

950–990 cm^{-1})[22] normally observed in dimeric di-μ-oxo-oxomolybdates(V) and monooxo complexes. Similar effects were observed in the case of *trans*-dioxo complexes of Re(V), Ru(VI), and Os(VI).[23] The marked decrease of the metal–oxygen stretching force constants in the latter group of complexes was explained in terms of the strong trans interaction of π-bonded oxygen atoms. From these results and from the existence of tetrameric oxobromomolybdates(V) in solutions[24] we have assumed a model of these tetrameric oxomolybdates(V) shown in Figure 6. The assumed model of the tetrameric oxomolybdates (V) explains the analytical, magnetic, and infrared spectral data obtained.

Because the characteristic frequencies of the

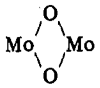

cores present in the tetrameric complexes remain unchanged if compared with those observed in the di-μ-oxo-oxomolybdates(V), a normal-coordinate analysis for the isolated O–Mo–O–Mo–O chain was possible assuming the $D_{\infty h}$ symmetry of the molybdenum–oxygen chain. The internal coordinates of this system are defined in Figure 7. Of the 10 modes of vibrations possible, 6 are infrared active ($2\ A_{1u} + 2\ E_{1u}$) and 4 are Raman active ($2\ A_{1g} + E_{1g}$). The vibrations of E_{1g} and E_{1u} symmetries correspond to the deformation modes of vibration of the Mo_2O_3 chain. The symmetry coordinates for the ir-active vibrations are given in Appendix B. It is noteworthy that the G-matrix elements are independent on the bond distances in the Mo_2O_3 chain. The results of calculations are shown in Table IX.

Table IX. Calculated and Observed Vibrational Frequencies of the Linear Mo_2O_3 Chain[a]

Sym of vibration	ν_{calcd}	ν_{exptl}	Type of vibration	Force constants,[b] mdyn/Å
A_{1u}'	718	720	S_2	$f^2{}_r = 3.78$
A_{1u}	881	885	S_1	$f^1{}_r = 4.24$

[a] Frequencies are given in cm^{-1}. [b] $f^1{}_r$ and $f^2{}_r$ correspond to the molybdenum–oxygen(terminal) and molybdenum–oxygen(bridge) stretching force constants, respectively. The stretch–stretch interaction force constants were assumed to be $f_{rr} = 0.1 f_r$.

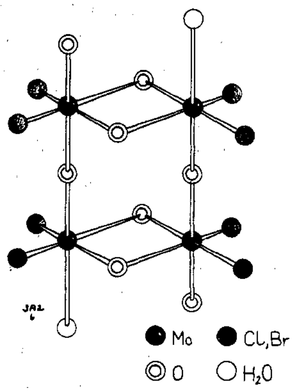

Figure 6. Structure of the di-μ-oxo-bis(di-μ-oxo-oxoaquotetrahalodimolybdate(V)) ion.

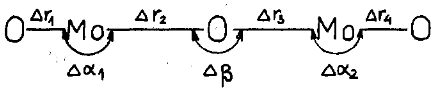

Figure 7. Internal coordinates of the O–Mo–O–Mo–O chain.

Discussion

Ir Spectra of Bi- and Tetranuclear Di-μ-oxo- and Di-μ-oxo-bis(di-μ-oxo)-Bridged Oxomolybdates(V). The ir spectra of dimeric di-μ-oxo-oxomolybdates(V) and of the corresponding monomeric oxomolybdates(V)[22a,d] differ considerably. In the spectra of all of the di-μ-oxo-oxomolybdates(V) two additional absorption bands due to the stretching vibrations of the four-membered planar Mo_2O_2 ring are present. Theoretical calculations show that these absorptions, observed in the ranges 470–520 and 730–740 cm^{-1}, are due to the stretching vibrations of A_u and B_u symmetries, respectively.

The calculated stretching force constants of the Mo–O_b bonds indicate a significant contribution of p_π–d_π bonding in the di-μ-oxo cores. This contribution is slightly smaller if compared with those observed for linear μ-oxo-bridged complexes. In linear μ-oxo cores the metal–oxygen(bridge) stretching force constants were found to be equal to 3.48–3.73 mdyn/Å. The calculated values of the Mo–O_{H_2O} and Mo–Cl(Br) stretching force constants indicate the existence of a considerable trans interaction of the "molybdenyl" oxygen atom on the Mo–O_{H_2O} bonds and a slight trans interaction of the bridging oxygen atoms on the Mo–Cl(Br) bonds. The metal–chloride stretching force constants are usually observed in the range 1.6–2.0 mdyn/Å for chloro complexes.[25] The values of the metal–bromide stretching force constants are normally 5–10% lower if compared with those for the

---

(22) (a) C. G. Barraclaugh, J. Lewis, and R. S. Nyholm, *J. Chem. Soc.*, 3552 (1959); (b) J. Selbin, L. H. Holmes, and S. P. McGlynn, *J. Inorg. Nucl. Chem.*, 25, 1359 (1963); (c) D. Brown, *J. Chem. Soc.*, 4944 (1964); (d) A. Sabatini and R. Bertini, *Inorg. Chem.*, 5, 204 (1966).

(23) (a) W. P. Griffith, *J. Chem. Soc.*, 245 (1964); (b) N. P. Johnson, C. J. Lock, and G. Wilkinson, *ibid.*, 1054 (1964); (c) M. Freni, D. Giusto, and P. Romiti, *Gazz. Chim. Ital.*, 97, 833 (1967); (d) W. P. Griffith and T. D. Wickins, *J. Chem. Soc. A*, 400 (1968).

(24) (a) B. Jezowska-Trzebiatowska and M. F. Rudolf, *Rocz. Chem.*, 42, 1221 (1968); (b) M. F. Rudolf, Ph.D. Thesis, Wroclaw, 1970; (c) B. Jezowska-Trzebiatowska and M. F. Rudolf, *Trans. Roy. Inst. Technol., Stockholm*, No. 258, 143 (1972).

(25) (a) J. R. Beattie, T. R. Gilson, and G. A. Ozin, *J. Chem. Soc. A*, 2770 (1968); (b) G. A. Ozin, G. W. Fowles, D. J. Tidmarsh, and R. A. Walton, *ibid.*, 644 (1969).

chloro complexes.[26] The stretching force constants of the Mo-O_b bonds in examined di-μ-oxo-oxomolybdates(V) remain unchanged if compared with those observed in all monooxo cations.[22]

As shown in the previous section, the ir spectra of the tetrameric oxomolybdates(V) may be interpreted on the bases of the geometrical configurations of the tetramers, which indicate the existence of bridge cores of the di-μ-oxo-bis(di-μ-oxo) type (Figure 6). Only such a model where single, strongly trans-interacting oxygen bridges are present could explain the absence of the "molybdenyl" stretching frequency normally observed in the monomeric and dimeric oxomolybdates(V). The frequency analysis of the proposed linear Mo_2O_3 chain predicts the existence, with exception of the stretching vibration at *ca.* 880 cm^{-1}, of a second stretching vibration in the region of *ca.* 720 cm^{-1}. This vibration is observed as a strong absorption in all tetrameric oxomolybdates(V) investigated (Table IV). The characteristic frequencies due to the Mo-O_b, Mo-O_{H_2O}, and Mo-Cl(Br) stretching modes of the di-μ-oxo-bridged units of the tetramers remain practically unchanged. This justifies the simplified treatment of the tetrameric $Mo_4O_8^{4+}$ core vibrations as in fact being due to the independent $Mo_2O_4^{2+}$ di-μ-oxo core and $Mo_2O_3^{4+}$ chain vibrations. The bond orders and bond lengths of Mo-O bonds in studied oxomolybdates(V) were determined on the basis of calculated force constants and also of X-ray data, bond orders, and force constant values of molybdenum-oxygen bonds reported in literature.[6-10,27-30] The results obtained are shown in Table X.

From the results given in Table X it follows that the bond order of the Mo-O_b bond in the di-μ-oxo cores in the bi- and tetranuclear oxomolybdates(V) amounts to 1.3 approximately. Hence the di-μ-oxo type bond should be considered as the intermediary case between the bonding observed in μ-oxo cores (formal bond order amounts to 1.5) and the simple σ metal-oxygen bonding.

In the case of tetrameric oxomolybdates(V) a marked decrease of the formal bond orders of the terminal molybdenum-oxygen bonds up to 1.7 (stretching force constant equal to 4.24 mdyn/Å) is observed. This value is much smaller if compared with the formal bond order of terminal Mo-O bonds in monomeric and dimeric di-μ-oxo-oxomolybdates(V). Similarly the stretching force constant value of the single-bridged molybdenum-oxygen bond is 3.78 mdyn/Å, exceeding markedly the force constant usually observed in μ-oxo-complexes.[30] This effect may be explained only in terms of the mutual strong trans interaction of the terminal and single-bridge oxygen atoms in the Mo_2O_3 chains of the tetramers. This effect leads to a considerable electron density delocalization along the O-Mo-O-Mo-O chains. As a result the pseudo *trans*-dioxo cationic groups are formed.

Ir Spectra of μ-Oxo- and Hetero-Bridged Oxomolybdates(V). The Sulfato, Perchlorato, and Oxalato Anions as Bridging Ligands. The ir spectrum of the pyridinium μ-oxo-bis(oxotetrakis(isothiocyanato)molybdate(V)) exhibits a characteristic absorption band at 868-873 cm^{-1} indicating the presence of a linear single oxygen bridge in this dimer.

Table X. Force Constants, Formal Bond Orders, and Predicted Bond Distances of the Molybdenum-Oxygen Bonds in Dimeric and Tetrameric Oxomolybdates(V)[a]

Compd	Bonding	Force constant, mdyn/Å	Formal bond order	Bond length, Å
$[Mo_2O_4Cl(Br)_4(H_2O)_2]^{2-}$	Mo-O_t	7.68	2.5	1.7
	Mo-O_b	3.10	1.3	1.95
	Mo-O_{H_2O}	1.05	1.0	2.2-2.3
	Mo-Cl	1.60		
	Mo-Br	1.48		
$[Mo_4O_8Cl(Br)_8(H_2O)_2]^{4-}$	Mo-O_t	4.24	1.7	1.83
	Mo-O_b	3.10	1.3	1.95
	Mo-O_b	3.78	1.5	1.90[b]

[a] The formal bond orders and predicted bond lengths were determined using the plots of dependences of the Mo-O formal bond orders and bond distances *vs.* Mo-O stretching force constants.[30] [b] These values correspond to the single molybdenum-oxygen bridge in linear Mo_2O_3 chains of tetramers.

In the hetero-bridged oxomolybdates(V) the sulfato and perchlorato anions do in fact function as bidentate ligands as suggested by the analytical data and clearly demonstrated by the ir spectra (Table V).

Until now the ir spectra of sulfato-bridged $[Co_2(NH_2,SO_4)(NH_3)_8]^{3+}$ and $[Pd(NH_3)_2SO_4]_n$ complexes were reported by Nakamoto, *et al.*,[31] and Eskenazi, *et al.*[32] Also some results concerning the ir spectra of bidentate tetrahedral oxoanions were reported by Barraclaugh, *et al.*,[33] and Coomber, *et al.*[34]

On coordination of a tetrahedral anion, *e.g.*, sulfato or perchlorato, as a bidentate or bridging ligand, its local symmetry is lowered to C_{2v}. From the correlation table of the T_d point group it follows that in C_{2v} symmetry all of the MO_4 ligand vibrations are Raman and infrared active. For the bidentate MO_4 ligand ν_1 should be infrared active, ν_2 should split into a doublet, and ν_3 and ν_4 should be split into triplets. The most characteristic trait of the C_{2v} distortion is the splitting of the intense $\nu_3(T_d)$ vibration into a triplet. As shown in Table V well-defined, sharp splittings of the ν_3 vibrations are really observed in the $(PyrH)_4[Mo_2O_3(SO_4)(NCS)_6]$ and $(PyrH)_3[Mo_2O_3(ClO_4)(NCS)_6]$ complexes indicating that these MO_4 ligands are acting as bidentate. Although the possibility of the presence of simple chelate sulfato or perchlorato groups in the $[Mo_2O_3(MO_4)(NCS)_6]^{m-}$ complexes should be taken into account, the resulting nonequivalency of two molybdenum atoms in these dimers would be unjustified. Besides that, the ir spectra in the Mo-O_b stretching frequency region of such complexes should be nearly close to that of the $[Mo_2O_3(NCS)_8]^{4-}$ complex in contrast with the results given in Table V.

Therefore we prefer the presence of bridging sulfato or perchlorato ligands in the $[Mo_2O_3(MO_4)(NCS)_6]^{m-}$ complexes. That the MO_4 anions are bridging ligands is confirmed additionally by the synthesis route of these complexes in which no NCS^- ligand elimination from the starting $(PyrH)_4[Mo_2O_4(NCS)_6]$ complex was observed.

The Mo-O_t stretching frequency in the μ-sulfato- and μ-perchlorato-μ-oxo-oxodimolybdates(V) remain unchanged if compared with those of the starting $[Mo_2O_4(NCS)_6]^{4-}$ ion. But remarkable differences are observed in the region of Mo-

---

(26) (a) R. J. H. Clark, *Spectrochim. Acta*, 21, 955 (1965); (b) D. M. Adams and P. J. Chandler, *Chem. Commun.*, 69 (1966).

(27) A. B. Blake, F. A. Cotton, and J. S. Wood, *J. Amer. Chem. Soc.*, 86, 3024 (1964).

(28) F. A. Cotton, S. M. Morehouse, and J. S. Wood, *Inorg. Chem.*, 3, 1603 (1964).

(29) F. A. Cotton and R. C. Elder, *Inorg. Chem.*, 3, 397 (1964).

(30) F. A. Cotton and R. M. Wing, *Inorg. Chem.*, 4, 867 (1965).

(31) (a) K. Nakamoto, J. Fujita, S. Tanaka, and M. Kobayashi, *J. Amer. Chem. Soc.*, 79, 4904 (1957); (b) K. Nakamoto, "Infrared Spectra of Inorganic and Coordination Compounds," Wiley, New York, London, 1963, p 165.

(32) R. Eskenazi, J. Raskovan, and R. Levitus, *J. Inorg. Nucl. Chem.*, 28, 521 (1966).

(33) C. G. Barraclaugh and M. L. Tobe, *J. Chem. Soc.*, 1993 (1961).

(34) R. Coomber and W. P. Griffith, *J. Chem. Soc. A*, 1129 (1968).

O_b stretching frequencies. For the μ-sulfato- and μ-perchlorato-bridged species a decrease of the frequency corresponding to the A_u (435 and 443 cm^{-1}, respectively) and increase of the frequency corresponding to the B_u (785 cm^{-1} in both complexes) stretching vibrations of the Mo–O_b bonds in comparison with the appropriate values found in the $[Mo_2O_4(NCS)_6]^{4-}$ complex are observed. This may be explained easily as due to the Mo–O_b–Mo bond angle increasing, resulting after the SO_4 and ClO_4 bridge formation. Similar dependences of the symmetric and asymmetric stretching frequencies on the bond angle were observed in several single-bridged binuclear complexes.[35,36]

The N-coordination of the SCN^- ligand in all investigated complexes may be easily deduced from the characteristic values of the ν(C≡N), ν(Mo–N) stretching, and δ(NCS) deformation frequencies given in Tables III and V. Similar values of the appropriate vibration frequencies were observed in several isothiocyanato complexes,[37-40] and therefore no further discussion of this is necessary.

Electronic Structure and Metal-Metal Bond in Polynuclear Oxygen-Bridged Oxomolybdates(V). As was shown in Table II, all dimeric di-μ-oxo-oxomolybdates(V) studied are diamagnetic or exhibit only a small, nearly temperature-independent paramagnetism in the range of (100–300) × 10^{-6} cgsu. Because of the short Mo–Mo distance, due to the presence of di-μ-oxo bridges both the bonding interaction through the oxygen bridges and the metal-metal bonding should be of significance. The existence of direct metal-metal bonds in di-μ-oxo-oxomolybdates(V) was suggested for the first time by Cotton, *et al.*,[8] because of the short Mo–Mo distance 2.541 Å observed in the diamagnetic potassium di-μ-oxo-bis(oxooxalatoaquomolybdate(V)). Similar Mo–Mo distances were determined by Prout, *et al.*,[9,10] in L-histidine and cysteine complexes of molybdenum(V).

To explain the magnetic properties of di-μ-oxo-oxomolybdates(V) and to determine the role of molybdenum-molybdenum interactions in that group of complexes, the theoretical calculations of electronic structure of the $[Mo_2O_4Cl_4(H_2O)_2]^{2-}$ ion, as the most typical of that group, were carried out. With regard to molybdenum-nonbridge (O_t, H_2O, Cl) atom interactions only, the splitting of d orbitals of molybdenum into two main groups was observed. Four orbitals originating from octahedral e_g orbitals are located considerably higher, and six orbitals originating from octahedral t_{2g} orbitals are located much lower. Their energy is connected with molybdenum-ligand π interaction.

Consideration of the molybdenum-bridge oxygen interaction (Figure 2B) led to the following energy ordering of the MO's: $b_u(xy) < a_g(xz,yz) \sim a_g(xy) < a_u(xz,yz) < b_g(xz,yz) \sim b_u(xz,yz) \ll b_g(x^2-y^2) \ll b_u(z^2) \sim a_u(x^2-y^2) < a_g(z^2)$

In the last stage of the calculations we have considered the metal-metal interaction, which exhibits complex character (Figure 2C). In the group of the σ-antibonding orbitals it has the character of π–π and δ-δ interactions, with no essential influence on orbital energy. In the group of π-antibonding molybdenum orbitals the metal-metal interaction has the essential influence on energy ordering of orbitals. As a result of this interaction, mainly of the σ type, the orbitals $a_g(xy)$ and $b_u(xy)$ are bonding and antibonding, respectively. Since the orbital $a_g(xy)$ is occupied by two electrons, the molybdenum-molybdenum bond formation through d_{xy} orbitals is the factor responsible for the further stabilization of a complex and for the magnetic properties of that system.

The highest occupied orbital $a_g(xy)$, originating from molybdenum d orbitals, is occupied by two electrons. Therefore the ground state of the $[Mo_2O_4Cl_4(H_2O)_2]^{2-}$ complex is the orbital singlet ^1A_g. Since the energy distance between the $a_g(xy)$ orbital and the next $a_u(xz)$ orbital exceeds 6000 cm^{-1} (see Table VI), the contribution of the excited triplet states $^3A_u[a_g(xy)^1\ a_u(xz)^1]$, responsible for temperature-dependent paramagnetism, has to be excluded. Therefore the di-μ-oxo-bis(oxodichloroaquomolybdate(V)) complex ion should be diamagnetic or exhibit only a small temperature-independent paramagnetism. This conclusion is in excellent agreement with the experimental results. The results obtained for the $[Mo_2O_4Cl_4(H_2O)_2]^{2-}$ complex may be transferred about the whole group of studied dimeric di-μ-oxo-oxomolybdates(V).

In a similar way the almost complete reduction of the magnetic moment in tetranuclear di-μ-oxo-bis(di-μ-oxo-oxodimolybdates(V)) obtained by us may be explained. Their basic structural units are, as shown above, the $Mo_4O_8^{4+}$ cores. The results of ir spectra indicate that the geometric structure, bond orders, bond lengths, and bond angles of doubly bridged fragments of $Mo_4O_8^{4+}$ cores are the same as in the $Mo_2O_4^{2+}$ cores (see Tables III, IV). Thus, the spin quenching within the $Mo_4O_8^{4+}$ cores should be explained similarly as for the di-μ-oxo cores, by the formation of strong, single σ molybdenum-molybdenum bonds.

In our prior paper concerning the complexes with linear oxygen bridges we have explained the cause of the diamagnetism and of the singlet-triplet equilibria of $[M_2OL_{10}]^{m-}$ ions, where M = Os(IV), Re(IV), Ru(IV), or Cr(III) and L denotes σ-bonding or weak π-donating ligands.[41] We have reported also that the tetragonal structure D_{4h} with a linear bridge is attainable for central atoms having not more than four d electrons. For d^5 electronic structure the bent bridge bonding should be expected. Such a structure is really observed in some iron(III) complex compounds.[42] In the series of μ-oxo-bridged dimeric oxomolybdates(V) all of the studied complexes exhibit only a small temperature-independent paramagnetism in the range of (150–200) × 10^{-6} cgsu. A small paramagnetism, of the same order of magnitude, was observed previously in the μ-oxo-bis(oxobis(ethyl xanthato)-molybdate(V))[27] and cesium μ-oxo-bis(oxotetrachloromolybdate(V)).[43] The studied pyridinium μ-oxo-bis(oxotetrakis(isothiocyanato)molybdate(V)) also falls into this class of complexes. The electronic structure calculations of the $[Mo_2O_3(NCS)_8]^{4-}$ complex carried out by the angular overlap method have proved that the energetically lowest orbital became $b_g(yz)$ and the term $^1A_g[b_g(yz)^2]$ is the ground term for the d^1-d^1 configuration. The next group of close orbitals—$a_g(xz)$, $a_u(yz)$, a_u,$b_g(xy)$—is π antibonding because of the interaction with bridge or terminal oxygen atoms. The energy distance $\Delta E[a_g(xz)$-$b_g(yz)]$, expressed in terms of AOM parameters, is close to $e^t_\pi - e^L_\pi$ (Table VIII, Figure 4). This value corresponds to the separation of the e(xz,yz) and $b_2(xy)$ orbitals in a monomeric $[MOL_5]^{n-}$ chromophore

---

(35) D. J. Hewkin and W. P. Griffith, *J. Chem. Soc. A*, 472 (1966).

(36) B. Jezowska-Trzebiatowska, J. Hanuza, and W. Wojciechowski, *Spectrochim. Acta*, 23, 2631 (1967).

(37) J. Lewis, R. S. Nyholm, and P. W. Smith, *J. Chem. Soc.*, 4950 (1961).

(38) A. Sabatini and I. Bertini, *Inorg. Chem.*, 4, 959 (1965).

(39) R. A. Bailey, S. L. Kozak, T. W. Michelsen, and W. N. Mills, *Coord. Chem. Rev.*, 6, 407 (1971).

(40) H. Sabat, M. F. Rudolf, and B. Jezowska-Trzebiatowska, *Inorg. Chim. Acta*, in press.

(41) B. Jezowska-Trzebiatowska, H. Kozlowski, and L. Natkaniec, *Bull. Acad. Polon. Sci., Ser. Sci. Chim.*, 19, 115 (1971).

(42) A. Earnshaw and J. Lewis, *J. Chem. Soc.*, 396 (1961).

(43) R. Colton and C. G. Rose, *Aust. J. Chem.*, 21, 883 (1968).

of C_{4v} symmetry. As shown by us for oxoisothiocyanatomolybdates(V) $[MoO(NCS)_5]^{2-}$, this separation is equal to 12,600 cm^{-1}.[40] The energy separations of the $a_u(yz)$ and $b_g,a_u(xy)$ orbitals from the energetically lowest $b_g(yz)$ orbital in the dimer are equal to $e^b{}_\pi$ and $e^t{}_\pi$, respectively. Because of the smaller π interaction of the bridging oxygen atom with the molybdenum atoms, if compared with those for the terminal oxygen atoms, the sequence $e^b{}_\pi < e^t{}_\pi$ of the appropriate AOM parameters is easily deduced. Therefore the first excited molybdenum orbital corresponds to the $a_u(yz)$ orbital. The energy distance between the $a_u(yz)$ and $b_g(yz)$ orbitals is not smaller if compared with the separation of the $e_u(xz,yz)$ and $b_{2g}(xy)$ orbitals in a $[L_5M{-}O{-}ML_5]^{m-}$ chromophore (see also ref 41). Hence it follows that the ground term of the $[Mo_2O_3(NCS)_8]^{4-}$ complex ion is the orbital singlet $^1A_g[b_g(yz)^2]$. The energy distance between the first excited triplet term $^3B_u[b_g(yz)^1\ a_u(yz)^1]$ must be at least 10,000 cm^{-1}. Therefore the contribution of excited triplet states and their influence on the magnetic properties of dimeric μ-oxo-bridged oxoisothiocyanatomolybdates(V) must be ruled out. This conclusion seems be valid also in the case of isostructural dimeric chloro- and (ethyl xanthato)oxomolybdates(V).

Also in the series of hetero-bridged binuclear oxomolybdates(V) only a slight paramagnetism was observed. The slight temperature dependence of the magnetic susceptibility observed in some cases may be due to small amounts of paramagnetic impurities in the samples. Taking into account that the sulfato-, perchlorato-, and oxalato-bridging ligands are bidentate, the considerable increase of the molybdenum-molybdenum distance should be expected.[44] That must result in the weakening of the direct Mo-Mo bonding in comparison with those observed in $Mo_2O_4{}^{2+}$ cores. In any complex of that group the increase of the magnetic susceptibility with increasing temperature, in spite of the direct metal-metal bonding being weakened, was not observed.

The hetero-bridged species may be considered as intermediate to the linear Mo-O-Mo systems and the four-membered ring systems. Because of the direct Mo-Mo bond cleavage, the energy level diagram of the hetero-bridged species should correspond roughly to Figure 2B (Mo_2O_2 ring system without Mo-Mo interaction) and the energy distance between the two low-lying d orbitals should be sufficient to provide the total spin pairing.

The results presented in this paper confirm the frequent occurrence of oxygen bridges in complexes of the quinquivalent molybdenum. The double oxygen bonding also allows the presence of direct metal-metal bonds which, in the case of discussed complexes, effects strongly their magnetic properties.

Acknowledgment. This work was supported by a financial grant from the Polish Academy of Sciences.

Appendix A. Symmetry Coordinates for Ir-Active Vibrations of the $[Mo_2O_4(hal)_4(H_2O)_2]^{2-}$ Complexes

A_u species

$S_1 = {}^1\!/_2(\Delta r_1 - \Delta r_2 - \Delta r_3 + \Delta r_4)$
$S_2 = {}^1\!/_2(\Delta s_1 - \Delta s_2 + \Delta s_3 - \Delta s_4)$
$S_3 = {}^1\!/_2(\Delta\beta_{11} - \Delta\beta_{21} + \Delta\beta_{34} - \Delta\beta_{44})$
$S_4 = {}^1\!/_2(\Delta\beta_{13} - \Delta\beta_{23} + \Delta\beta_{32} - \Delta\beta_{42})$
$S_5 = {}^1\!/_2(\Delta\delta_{12} - \Delta\delta_{22} - \Delta\delta_{33} + \Delta\delta_{43})$
$S_6 = {}^1\!/_2(\Delta\delta_{14} - \Delta\delta_{24} - \Delta\delta_{31} + \Delta\delta_{41})$

B_u species

$S_7 = {}^1\!/_2(\Delta r_1 + \Delta r_2 - \Delta r_3 - \Delta r_4)$
$S_8 = {}^1\!/_2(\Delta s_1 + \Delta s_2 - \Delta s_3 - \Delta s_4)$
$S_9 = (1/\sqrt{2})(\Delta t_1 - \Delta t_4)$
$S_{10} = (1/\sqrt{2})(\Delta t_2 - \Delta t_3)$
$S_{11} = (1/\sqrt{2})(\Delta\alpha_{12} - \Delta\alpha_{34})$
$S_{12} = {}^1\!/_2(\Delta\beta_{11} + \Delta\beta_{21} - \Delta\beta_{34} + \Delta\beta_{44})$
$S_{13} = {}^1\!/_2(\Delta\beta_{13} + \Delta\beta_{23} - \Delta\beta_{32} - \Delta\beta_{42})$
$S_{14} = (1/\sqrt{2})(\Delta\gamma_{12} - \Delta\gamma_{34})$
$S_{15} = {}^1\!/_2(\Delta\delta_{12} + \Delta\delta_{22} - \Delta\delta_{33} - \Delta\delta_{43})$
$S_{16} = {}^1\!/_2(\Delta\delta_{14} + \Delta\delta_{24} - \Delta\delta_{31} - \Delta\delta_{41})$

Appendix B. Symmetry Coordinates of the Ir-Active Vibrations of the Mo_2O_3 Chain

A_{1u} species

$S_1 = (1/\sqrt{2})(\Delta r_1 - \Delta r_4)$
$S_2 = (1/\sqrt{2})(\Delta r_2 - \Delta r_3)$

E_{1u} species

$S_3 = \beta$
$S_4 = \beta'$
$S_5 = (1/\sqrt{2})(\Delta\alpha_1 + \Delta\alpha_2)$
$S_6 = (1/\sqrt{2})(\Delta\alpha_1{}' + \Delta\alpha_2{}')$

Registry No. IV, 43111-83-7; V, 43065-28-7; VI, 43111-84-8; VII, 43111-85-9; VIII, 43111-86-0; IX, 43065-23-2; X, 43065-22-1; XI, 43065-24-3; XII, 43065-25-4; XIII, 22323-42-8; XIV, 43111-88-2; XV, 43111-89-3; XVI, 43111-90-6; XVII, 43111-91-7; $K_2[Mo_2O_4(C_2O_4)_2(H_2O)_2]\cdot 3H_2O$, 43111-92-8; $[Mo_2O_4Cl_4(H_2O)_2]^{2-}$, 41754-99-8; $[Mo_2O_4Br_4(H_2O)_2]^{2-}$, 43065-29-8; $[Mo_4O_8Cl_8(H_2O)_2]^{4-}$, 43065-26-5; $[Mo_4O_8Br_8(H_2O)_2]^{4-}$, 43065-27-6.

---

(44) As shown by U. Thewalt, *Acta Crystallogr., Sect. B*, **27**, 1744 (1971), the Co-Co distance in the sulfato-bridged $[Co_2(SO_4,NH_2)(en)_4]Br_3$ complex is equal to 3.510 Å.